ELSEVIER

Journal of Photochemistry and Photobiology A: Chemistry 123 (1999) 67–76

Journal of Photochemistry and Photobiology A:Chemistry

Excitation energy transfer and photo-induced electron transfer in axial bispyrenyl phosphorus porphyrin derivatives: factors governing the competition between energy and electron transfer processes under the existence of intramolecular π–π interaction

Kazutaka Hirakawa[a], Hiroshi Segawa[a,b,*]

[a]*Graduate School of Arts and Sciences, The University of Tokyo, 3-8-1 Komaba, Meguro-ku, Tokyo 153-8902, Japan*
[b]*CREST Sasabe Project, Japan Science and Technology Corporation, 3-8-1 Komaba, Meguro-ku, Tokyo 153-8902, Japan*

Received 24 November 1998; received in revised form 2 February 1999; accepted 17 February 1999

Abstract

In order to investigate the competition between energy and electron transfer processes, pyrene–phosphorus(V)porphyrin triads in which two pyrenes are connected to a central phosphorus atom through various bridges were synthesized. The triads have π–π interaction between the pyrene and the porphyrin moieties. As a result, emissions from the photo-excited states of pyrene and porphyrin were quenched through energy and/or electron transfer processes. In the relaxation from the excited state pyrene, the predominant process changed according to solvents and donor–acceptor distances.

Keywords: Energy; Electron transfer; Triads; Pyrene; Porphyrin

1. Introduction

Photo-induced electron transfer and excitation energy transfer are essential processes of natural photosynthesis [1–4]. Biological organisms, as photosynthetic reaction centers and light harvesting complexes, ingeniously use photophysical processes to achieve significantly high efficiency in total photoenergy conversion. To the best of our knowledge, the molecular systems in these organisms are the highest class of molecular photodevices. In order to realize artificial molecular systems for photoenergy conversion and photo-electronic operation, natural photosynthetic systems are very useful examples, and various mimetic systems containing porphyrins have been synthesized to investigate the photophysical processes involved [5–7]. One of the key factors governing these processes is the interaction between a donor (D) and an acceptor (A) of energy and/or electron. For porphyrin molecular systems, various donor–acceptor (D–A) systems have been investigated so far as energy and electron transfer models in which, due to the synthetic demand of rigid models, the intramolecular interactions are usually changed in the inter-planer directions of the porphyrins [5–25]. Since the π-orbital of an aromatic ring generally spreads in its axial direction, the intramolecular D–A interaction of the porphyrin ring should also be changed in the axial direction to allow investigation of the π-orbital interaction. A phosphorus porphyrin is very useful for this purpose because various compounds can be connected at a central phosphorus atom and model compounds can be constructed to investigate the interaction in the axial direction [26–31].

In this study, we synthesized a series of pyrene–porphyrin triads in which two pyrene moieties were connected at the central phosphorus atom of phosphorus porphyrin through various lengths of bridges, investigating the interaction between the pyrene and the porphyrin moieties in the axial direction. The main reason for connecting two pyrenes to porphyrin is that energy transfer could be expanded to photoenergy harvesting [32,33]. In the triads, the pyrene moiety acts as both an electron and an energy donor. As a result, electron transfer is considered to compete with energy transfer from photo-excited pyrene [34]. Since electron transfer and energy transfer are selected perfectly in a natural photosynthetic system, factors concerning the selectivity between electron transfer and energy transfer need to be discussed. With respect to this point, we try to explain the selectivity using classical theories.

*Corresponding author. Tel.: +81-03-5454-6579; fax: +81-03-5454-6998; e-mail: csegawa@komaba.ecc.u-tokyo.ac.jp

1010-6030/99/$ – see front matter
PII: S1010-6030(99)00043-X

2. Experimental details

2.1. Measurement

^{1}H NMR spectra were taken on a JNM-A 500 (500 MHz) FT-NMR spectrometer (JEOL). Chemical shifts of ^{1}H were measured in δ (ppm) units relative to the tetramethylsilane (TMS) internal standard.

The absorption and emission spectra were taken on a V-570 UV/VIS/NIR spectrophotometer (JASCO) and a FP-777 spectrophotometer (JASCO), respectively. The fluorescence quantum yields of the porphyrin and the pyrene moieties of triads were determined relative to pyrene ($\Phi = 0.65$) [35] and $(CH_3O)_2$P(V)TPP ($\Phi = 0.044$) [29,30,36]. Fluorescence lifetimes were determined by a two-dimensional photon-counting technique using a streak camera (Hamamatsu, C4334 streakscope, time resolution: ca. 15 ps) and the excitation pulse source of a model-locked Ti-sapphire laser (Spectra Physics, Tsunami, frequency-doubled excitation pulse: 400 nm, FWHM: 200 fs). All the samples for the steady state and transient emission measurements were purged with nitrogen.

Cyclic voltammograms were measured with a three-electrode system using a platinum working, a platinum counter, and a saturated calomel reference electrode (SCE), which were assembled with a HABF501 potentiogalvanostat (HOKUTO DENKO). All the electrolysis solutions were purged with nitrogen.

2.2. Materials

The following substances were purchased from Aldrich: 1-hydroxypyrene, 1-pyrenemethanol, and 1-pyrenebutanol. Acetonitrile, dichloromethane, and toluene (spectroscopic analysis grade) were purchased from Dojin Chem. Ind. and used as received. Dichlorophosphorus(V)tetraphenylporphyrin chloride ($[Cl_2P(V)TPP]^+Cl^-$) [37], and dimethoxyphosphorus(V)tetraphenylporphyrin chloride ($(CH_3O)_2$P-(V)TPP) [26] were prepared according to previous reports.

2.2.1. Triad 1: Bis(1-pyrenoxy)phosphorus(V)-tetraphenylporphyrin chloride $[(C_{16}H_9O)_2P(V)\ TPP]^+Cl^-$

$[Cl_2P(V)TPP]^+Cl^-$ (0.100 g, 1.33×10^{-4} mol) and 1-hydroxypyrene (0.174 g) were dissolved in 5 ml of dry pyridine and refluxed at 115°C for 24 h. The reaction was supervised by absorption spectra and thin-layer chromatograph (TLC). As the axial ligands were exchanged, the reaction mixture turned from green to brown. At the end of the reaction, pyridine was removed by vacuum evaporation. The product was purified by column chromatography on neutral alumina with chloroform as an eluent and silica gel with chloroform–methanol (10/1, v/v), the result being a pure product in 47% (0.071 g) yield. ^{1}H NMR ($CDCl_3$, TMS): δ 1.62 (dd, 2H, $J_{H-H} = 8.5$ Hz, $J_{P-H} = 2.0$ Hz, pyrenyl-H), 3.85 (d, 2H, $J_{H-H} = 9.5$ Hz, pyrenyl-H), 6.66 (d, 2H, J_{H-H}=9.0 Hz, pyrenyl-H), 6.90 (d, 2H, $J_{H-H} = 9.5$ Hz, pyrenyl-H), 7.15 (br. s, 8H, *o*-meso-phenyl-H), 7.28 (t, 8H, $J_{H-H} = 5.5$, 8.0 Hz, *m*-meso-phenyl-H), 7.38 (d, 2H, $J_{H-H} = 9.0$ Hz, pyrenyl-H), 7.52 (t, 4H, $J_{H-H} = 8.0$ Hz, *p*-meso-phenyl-H), 7.64 (d, 2H, $J_{H-H} = 8.5$ Hz, pyrenyl-H), 7.68 (d, 2H, $J_{H-H} = 7.5$ Hz, pyrenyl-H), 7.77 (t, 2H, $J_{H-H} = 7.8$ Hz, pyrenyl-H), 7.91 (d, 2H, $J_{H-H} = 7.5$ Hz, pyrenyl-H), 9.04 (br. s, 8H, βH). FAB/MS: *m/z* 1077 (M^+). UV–Vis absorption spectrum in dichloromethane: λ_{max} ((nm) (log ε)), 336 (4.75), 352 (4.84), 429 (5.30), 564 (3.93).

2.2.2. Triad 2: Bis(1-pyrenemethoxy)-phosphorus(V)tetraphenylporphyrin chloride $[(C_{16}H_9CH_2O)_2P(V)TPP]^+Cl^-$

$[Cl_2P(V)TPP]^+Cl^-$ (0.120 g, 1.60×10^{-4} mol) and 1-pyrenemethanol (0.610 g) were dissolved in 2.5 ml of dry pyridine and refluxed at 100°C for 100 h. The reaction proceeded similarly and the reaction mixture was worked up in a similar manner. The pure product was obtained in 28% (0.051 g) yield. ^{1}H NMR ($CDCl_3$, TMS): δ −0.56 (d, 4H, $J_{P-H} = 16$ Hz, O-CH_2-pyrenyl), 4.99 (d, $J_{H-H} = 8.0$ Hz, 2H, pyrenyl-H), 5.13 (d, $J_{H-H} = 9.5$ Hz, 2H, pyrenyl-H), 7.20 (d, $J_{H-H} = 8.0$ Hz, 2H, pyrenyl-H), 7.26 (d, $J_{H-H} = 9.5$ Hz, 2H, pyrenyl-H), 7.52 (t, $J_{H-H} = 7.0$ Hz, 12 H, *m*, *p*-meso-phenyl-H), 7.61 (d, $J_{H-H} = 9.0$ Hz, 2H, pyrenyl-H), 7.67 ∼ 7.70 (m, 8H, *o*-meso-phenyl-H), 7.81 ∼ 7.87 (m, 6H, pyrenyl-H), 8.00 (d, $J_{H-H} = 6.5$ Hz, 2H, pyrenyl-H), 9.10 (d, $J_{P-H} = 3.0$ Hz, 8H, βH). FAB/MS: *m/z* 1105 (M^+). UV–Vis absorption spectrum in dichloromethane: λ_{max} (nm (log ε)), 316 (4.44), 330 (4.69), 346 (4.82), 432 (5.29), 562 (4.04), 602 (3.52).

2.2.3. Triad 3: Bis(1-pyrenebutoxy)phosphorus(V)-tetraphenylporphyrin chloride $[(C_{16}H_9(CH_2)_4O)_2P(V)TPP]^+Cl^-$

$[Cl_2P(V)TPP]^+Cl^-$ (0.050 g, 6.65×10^{-5} mol) and 1-pyrenebutanol (0.109 g) were dissolved in 5 ml of dry pyridine and refluxed at 115°C for 24 h. Except for the use of silica gel eluent (chloroform–methanol 19/1, v/v), the product was purified in a similar manner and obtained in 39% (0.032 g) yield. ^{1}H NMR ($CDCl_3$, TMS): δ −2.57 ∼ −2.52 (m, 4H, P-O-CH_2CCC-pyrenyl), −1.41 ∼ −1.38 (m, 4H, P-O-CCH_2CC-pyrenyl), −0.49 ∼ −0.43 (m, 4H, P-O-$CCCH_2$C-pyrenyl), 1.96 (t, 4H, $J_{H-H} = 8.0$ Hz, P-O-$CCCCH_2$-pyrenyl), 6.83 (d, 2H, $J_{H-H} = 7.5$ Hz, pyrenyl-H), 7.11 (d, 2H, $J_{H-H} = 9.5$ Hz, pyrenyl-H), 7.58 ∼ 7.63 (m, 12H, *m*, *p*-meso-phenyl-H), 7.69 (d, 2H, J_{H-H}=7.5 Hz, pyrenyl-H), 7.71 (d, 2H, $J_{H-H} = 9.5$ Hz, pyrenyl-H), 7.75 (d, 8H, $J_{H-H} = 7.5$ Hz, *o*-meso-phenyl-H), 7.83 (d, 2H, $J_{H-H} = 9.0$ Hz, pyrenyl-H), 7.95 (d, 2H, $J_{H-H} = 8.5$ Hz, pyrenyl-H), 7.97 (t, 2H, $J_{H-H} = 7.5$ Hz, pyrenyl-H), 8.08 (d, 2H, $J_{H-H} = 7.0$ Hz, pyrenyl-H), 8.13 (d, 2H, $J_{H-H} = 7.5$ Hz, pyrenyl-H), 8.84 (d, 8H, $J_{P-H} = 2.5$ Hz, βH). FAB/MS: *m/z* 1189 (M^+). UV–Vis absorption spectrum in dichloromethane: λ_{max} (nm (log ε)) 314 (4.50), 328 (4.72), 344 (4.84), 431 (5.40), 561 (4.12), 602 (3.59).

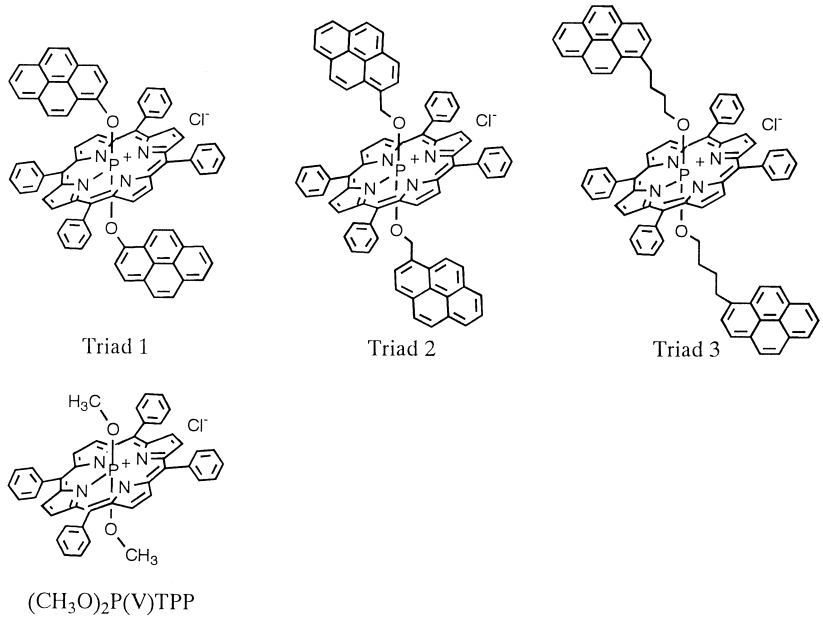

Fig. 1. Structure of pyrene–porphyrin Triads 1–3 and $(CH_3O)_2P(V)TPP$.

Table 1
Selected chemical shift data of ^{1}H-NMR for pyrene–porphyrin triads

Compound	Pyrenyl group								
	δ, ppm (position)								
Triad 1	1.62 (2)	3.85 (10)	6.66 (3)	6.90 (9)	7.38 (4)	7.64 (5)	7.68 (8)	7.77 (7)	7.91 (6)
Triad 2	4.99 (2)	5.13 (10)	7.20 (3)	7.26 (9)	7.61 (4)		7.81–7.87[a] (5, 8, and 7)		8.00 (6)
Triad 3	6.83 (2)	7.11 (10)	7.69 (3)	7.71 (9)	7.83 (4)	7.95 (5)	7.97 (8)	8.08 (7)	8.13 (6)

[a]Multiplet.

3. Results and discussion

3.1. General properties and intramolecular π–π interaction of triads

The three triads (Fig. 1) were different as regards the distance between the pyrene edge and the porphyrin center. By strong ring current effect of the porphyrin ring, all the ^{1}H-NMR signals of pyrene bonded to the porphyrin center shifted to a field higher than that of pyrene (Table 1). The ring current shifts of the protons increased with the shortening of the bridge length, indicating that their average distances between pyrenes and porphyrin are determined by the bridge length.

The π–π interaction between the pyrene and the porphyrin moieties could be evaluated from the absorption spectra of the triads. In some porphyrin derivatives with aromatic rings, changes in the absorption spectrum of porphyrin, such as bathochromic and hypochromic effects with spectral broadening were reported [38–40]. The absorption changes were interpreted by charge transfer through the π–π interaction. In the case of Triads 1–3, the absorption intensity decreased with the shortening of the bridge length (Fig. 2). In particular, Triad 1, with the shortest bridge among the triads, has quite a broad absorption spectrum in the Q band. Such a considerable change in the spectrum is specific for the interaction in the axial direction in pyrene–porphyrin systems [41].[1] Therefore, the spectrum of Triad 1 suggests strong π–π interaction through the direct contact of pyrene and porphyrin, as depicted in Fig. 3. For Triads 2 and 3, the spectral broadening could be explained on the basis of a thermal fluctuation with flapping contact in the partially overlapping area of the triads (Fig. 3). The absorption and

[1]5-(1-pyrenyl)-10,15,20-tri(*p*-methoxyphenyl)porphyrin derivatives in which one pyrene is bonding directly at the *meso* position of porphyrin were synthesized for the models to investigate the interaction between pyrene and porphyrin in the inter-planer direction. The absorption spectra of these compounds are almost the same as those of reference compounds (tetra(*p*-methoxyphenyl)porphyrin derivatives).

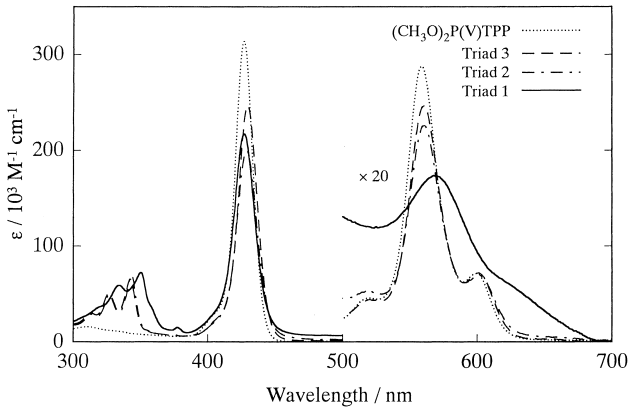

Fig. 2. Absorption spectra of Traids 1–3 and $(CH_3O)_2P(V)TPP$ in acetonitrile.

emission properties of Triads 1–3 and reference compounds are listed in Table 2. In the photo-excitation of the pyrene moieties of triads, neither excimer nor exciplex emissions were observed. Fluorescence quantum yields of the porphyrin (Φ_1) and the pyrene (Φ_2) moieties became remarkably smaller in the triads than in the corresponding reference compounds. These values suggest that the photo-excited states of the porphyrin and the pyrene moieties were quenched through energy and/or electron transfer.

To investigate the possibility of energy and/or electron transfer, the relationships of energy levels of excited pyrene, excited porphyrin, and the charge transfer (CT) state should be estimated. Redox potentials determined from the cyclic voltammogram (CV) of Triads 1–3, $(CH_3O)_2P(V)TPP$, and pyrenes are listed in Table 3. The oxidation potentials of

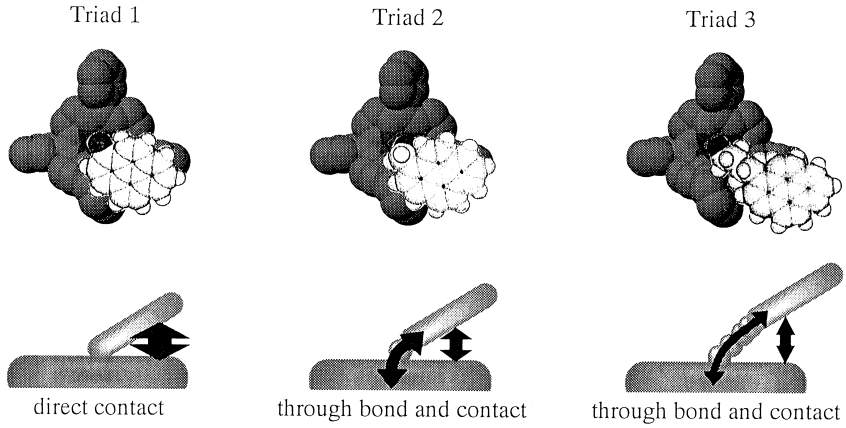

Fig. 3. Schematic representation of possible interactions between the pyrene and the porphyrin moieties in Triads 1–3.

Table 2
Photophysical properties of pyrene–porphyrin triads and reference compounds

Component	Solvent	Porphyrin				Pyrene			Pyrene → Porphyrin[a]
		Absorption		Emission		Absorption	Emission		
		Soret (nm)	Q (nm)	λ_{max} (nm)	$\Phi_1/10^{-2}$	λ_{max} (nm)	λ_{max} (nm)	$\Phi_2/10^{-2}$	$\Phi_3/10^{-2}$
Triad 1	CH_3CN	427	568	nd	–	334, 350	385, 407	0.008	–
	CH_2Cl_2	429	564	nd	–	336, 352	387, 407	0.007	–
	Toluene	433	567	609	0.008	338, 353	386, 406	0.011	nd
Triad 2	CH_3CN	429	560, 602	611, 659[b]	0.034	314, 327, 344	377, 395	0.11	trace
	CH_2Cl_2	432	562, 604	614, 667[b]	0.026	316, 330, 346	378, 398	0.11	trace
	Toluene	436	564, 604	612, 664[b]	0.69	316, 330, 348	378, 395	0.44	0.46
Triad 3	CH_3CN	430	560, 601	610, 664[b]	0.10	313, 326, 342	379, 396	0.12	trace
	CH_2Cl_2	431	561, 602	614, 668[b]	0.19	314, 328, 344	379, 396	0.093	trace
	Toluene	435	563, 603	610, 663[b]	0.98	316, 330, 346	377, 397	0.50	0.81
$(CH_3O)_2P(V)TPP$	CH_3CN	427	558, 599	612, 662[b]	4.4	–	–	–	–
	CH_2Cl_2	430	560, 601	614, 664[b]	4.4	–	–	–	–
	Toluene	434	563, 602	612, 667[b]	2.1	–	–	–	–
Pyrene	CH_3CN	–	–	–	–	306, 319, 334	373, 394	62	–
	CH_2Cl_2	–	–	–	–	308, 321, 337	374, 394	49	–
	Toluene	–	–	–	–	308, 322, 338	375, 394	52	–

[a] Φ_3 is the quantum yield of porphyrin fluorescence when the pyrene moieties are excited at 337 nm.
[b] Shoulder.

Table 3
Redox potentials of pyrene–porphyrin triads and reference compounds[a]

Compound	Reduction of porphyrin	Oxidation of pyrene	
	$E^{-}_{1/2}$ (V vs. SCE)	$E^{+}_{1/2}$ (V vs. SCE)	Anode peak (V vs. SCE)
Triad 1	−0.42 (x)	1.28 (x)[b]	1.35 (x)
Triad 2	−0.41 (y)	1.43 (y)[b]	1.50 (y)
Triad 3	−0.49 (x)	1.17 (x)[b]	1.24 (x)
$(CH_3O)_2$P(V)TPP	−0.50 (x)		
Pyrene	–	1.25 (x)	1.32 (x)
	–	1.20 (x)[c]	
	–	1.09 (y)[b]	1.16 (x)
1-hydroxypyrene	–	1.31 (x)[b]	1.38 (x)
1-pyrenemethanol	–	1.35 (y)[b]	1.42 (y)
1-pyrenebutanol	–	1.18 (x)[b]	1.25 (x)

[a] Cyclic voltammograms were measured in acetonitrile (x) or benzonitrile (y) solution with 0.1 M *n*-tetrabutoxyammonium perchlorate.
[b] $E^{+}_{1/2}$ was calculated by the subtraction of 0.07 V from the peak potential.
[c] From [42].

Triads 1 and 2 were more positive than the corresponding reference pyrenes (Table 3). These positive shifts of oxidation potentials indicate an electron donating character of the pyrene moieties in triads. In Triad 3, a very small difference was observed, indicating a weak interaction in the ground state for the long distance between pyrene and porphyrin. The energy levels of the CT states (E_{CT}) of Triads 1–3 in the solvents used for CV measurement (acetonitrile for Triads 1 and 3, benzonitrile for Triad 2) were estimated from the difference in the reduction potential of porphyrin and the oxidation potential of pyrene with ion-pair formation free enthalpy [43].[2] E_{CT} in the other solvents except for the CV measuring solvents is calculated by the dielectric continuum theory [43] from the redox potentials in the CV measuring solvents. Since the electron transfer reaction in Triads 1–3 is a pseudo charge-shift reaction as shown in Fig. 4, an ion-pair formed through electron transfer is composed of $[P^{+}Por^{-\bullet}–Py^{+\bullet}]^{+}$ and Cl^{-} counter ion. Therefore, ion-pair formation free enthalpy was estimated for the $[P^{+}Por^{-\bullet}–Py^{+\bullet}]^{+}Cl^{-}$ ion-pair. The estimated and calculated E_{CT} values are listed in Table 4 with the energy of the singlet excited states of pyrene (E^{py}_{S1}) and porphyrin (E^{por}_{S1}). As shown in Table 4, E_{CT} is lower than E^{por}_{S1} in acetonitrile and dichloromethane solutions. However, E_{CT} is very close to E^{por}_{S1} in toluene. These differences are caused by the stabilized energy of the CT states depending on solvent polarity. Schematic representations of the energy levels are given in Fig. 5. These relationships of energy levels suggest the possibility of controlling energy transfer and electron transfer processes by solvent polarity (described below).

3.2. Reductive photo-induced electron transfer from the excited state of porphyrin

Since the energy level of the phosphorus porphyrin HOMO is lower than those of the two pyrene HOMOs, reductive electron transfer from the ground state pyrene donors (D) to the excited porphyrin acceptor (A^{+*}) is expected to occur (process 1 in Fig. 5) when the porphyrin ring is photo-excited as given below.

$$[D–A^{+}–D] \xrightarrow{h\nu\,(560\,nm)} [D–A^{+*}–D] \xrightarrow{k^{por}_{elt}} [D–A^{\bullet}–D^{+\bullet}]$$

In this case, possibly, two charge-separated states with different $D^{+\bullet}$ are equivalent. The fluorescence quantum yields

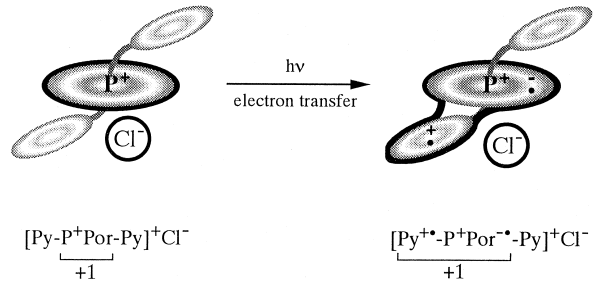

Fig. 4. Schematic representation of ionic interactions in charge transfer states in triads.

[2] In the excited CT state of Triads 1–3, a positive charged area is produced as shown in Fig. 4, so the interaction between the positive area and a chloride ion (counter ion of porphyrin) with the solvation of the positive area should be taken into account for the calculation. The CT state energy in solvent x (E_{CT})x was calculated from the following equation:

$$(E_{CT})_x = (E^{+}_{1/2} - E^{-}_{1/2}) + \frac{e^2}{2r}\left(\frac{1}{\varepsilon_x} - \frac{1}{\varepsilon_m}\right) - \frac{e^2}{\varepsilon_x a}$$

where $E^{+}_{1/2}$, $E^{-}_{1/2}$, e, ε_x, and ε_m are the half-wave one-electron oxidation and reduction potentials in solvent m, the electronic charge, and the static dielectric constants of solvent x and m, respectively. The effective ionic radii of positive area (r) are defined with the ionic radii of porphyrin (r_{por}), and one pyrene (r_{py}) with bridge length (r_{br}) as below:

$$r = \frac{(r_{por} + r_{py} + r_{br})}{2}$$

The estimated values are 7.18, 7.83, and 9.32 Å for Triads 1, 2, and 3, respectively. The distance a is the sum of r and Cl^{-} radius (1.81 Å). The following values were used as static dielectric constants: 36.0 (acetonitrile), 25.2 (benzonitrile), 7.77 (dichloromethane), and 2.38 (toluene), respectively.

Table 4
Estimated energy levels of pyrene–porphyrin triads in various solvents

Compound	Solvent	E_{S1}^{py} (eV)	E_{S1}^{por} (eV)	E_{CT} (eV)	$-\Delta G_0(^1Py^* \rightarrow CT)$ (eV)	$-\Delta G_0(^1Por^* \rightarrow CT)$ (eV)
Triad 1	CH_3CN	3.22	–	1.70	1.52	–
	CH_2Cl_2	3.20	–	1.70	1.50	–
	Toluene	3.21	2.04	1.83	1.38	0.21
Triad 2	CH_3CN	3.29	2.03	1.77	1.52	0.26
	CH_2Cl_2	3.28	2.02	1.79	1.49	0.23
	Toluene	3.28	2.03	1.95	1.33	0.08
Triad 3	CH_3CN	3.27	2.03	1.66	1.61	0.37
	CH_2Cl_2	3.27	2.02	1.70	1.57	0.32
	Toluene	3.29	2.03	1.92	1.37	0.11

E_{S1}^{py}: S1 energy of the pyrene moiety.
E_{S1}^{por}: S1 energy of the porphyrin ring.
E_{CT}: The CT state (pyrene$^{+\bullet}$–porphyrin$^{-\bullet}$) energy of the triads.

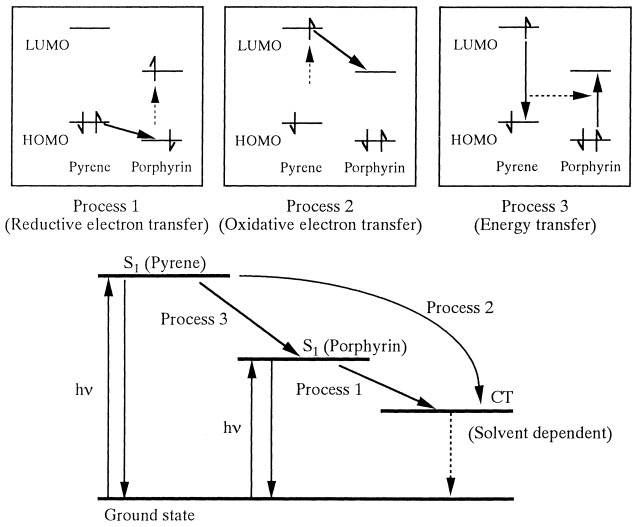

Fig. 5. Energy level relationships of the porphyrin and the pyrene moieties in the triads, and possible relaxation processes of the exicited states of the triads.

Φ_1 of the triads were smaller than those of $(CH_3O)_2P(V)TPP$ in any solvent (Table 2). Furthermore, Φ_1 became remarkably smaller as the pyrene–porphyrin distances were reduced (Table 2). These fluorescence quenchings were explained by electron transfer.[3] The electron transfer rate constant for porphyrin (k_{elt}^{por}) was calculated by the following equation:

$$k_{elt}^{por} = \frac{1}{2}\left(\frac{1}{\Phi_1} - \frac{1}{\Phi_0^{por}}\right)\frac{\Phi_0^{por}}{\tau_0^{por}} \quad (1)$$

where Φ_0^{por} and Φ_1 are the fluorescence quantum yields of the reference porphyrin and triads, respectively. The lifetimes of the singlet excited state (τ_0^{por}) of the reference porphyrin $(CH_3O)_2P(V)TPP$ were 5.6, 4.5, and 3.0 ns in acetonitrile, dichloromethane, and toluene, respectively. The dependencies of the obtained k_{elt}^{por} on the estimated pyrene–porphyrin center-to-center distances (d) and the solvent are shown in Fig. 6. The k_{elt}^{por} of Triad 1 is considerably large compared to those of Triads 2 and 3. The k_{elt}^{por} of the triads decreased with increasing d and depended on the solvent. Apparent attenuation coefficients (β value), which are roughly estimated from a few points in Triads 2 and 3, are 0.41 ± 0.20 Å^{-1}. The apparently small β values may have been caused by a thermal fluctuation with a partial interaction of the pyrene and the porphyrin moieties in Triad 3, wherein D–A interaction is caused not only by through bond but also by through space interaction with thermal

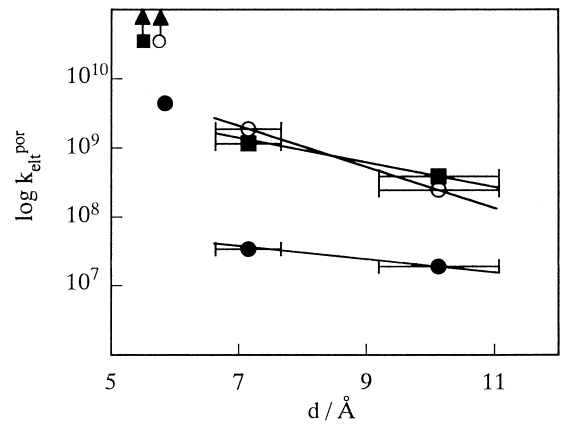

Fig. 6. The distance (d) dependence of the rate of electron transfer from ground state pyrene to the excited porphyrin moieties (k_{elt}^{por}) in acetonitrile (■), dichoromethane (○), and toluene (●).

[3]The formation of the radical pair was confirmed by transient absorption spectral measurements, where the absorption peaks ($\lambda_{max} = 690$ and 450 nm at 0.2 ps) were assigned to P(V)TPP$^{\bullet}$ and pyrene$^{+\bullet}$ (unpublished data), indicating the electron transfer from pyrene to excited porphyrin. Furthermore, the electron transfer rate constants (k_{elt}^{por}) estimated from the transient absorption spectra measurements were 7.0×10^{11} and 3.8×10^9 s^{-1} for Triads 1 and 3, respectively. These values are reasonable for values estimated from the fluorescence quantum yields.

motion as depicted in Fig. 3. Although the $-\Delta G_0$ (^{1}Por* → CT) of Triads 2 and 3 were in the normal region and different by a small value, the electron transfer rate in the relatively polar solvents, acetonitrile and dichloromethane were higher than those in toluene.[4] These results suggest that the electron transfer rates are controlled by the CT energy.

3.3. Oxidative photo-induced electron transfer and energy transfer from the excited state of pyrene

The emission from the pyrene moieties of Triads 1–3 were strongly quenched compared to the reference pyrene (Table 2). Fluorescence quenching is considered to be caused by electron transfer (process 2 in Fig. 5) and/or energy transfer (process 3 in Fig. 5) from excited pyrene (D^*) as given below:

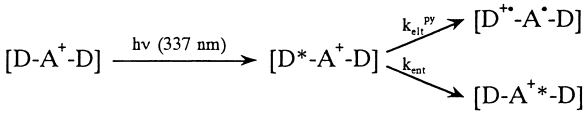

When energy transfer occurs, emission from porphyrin is observed by pyrene excitation, and a pyrene absorption structure is observed in the fluorescence excitation spectra of porphyrin emission. If these phenomena cannot be observed, only oxidative electron transfer quenching should be taken into account. As shown in Fig. 7, porphyrin emission was observed for Triads 2 and 3 when the pyrene moiety was excited at 337 nm, but not for Triad 1. The considerably weak emissions observed in acetonitrile and dichloromethane may have been caused by direct excitation of the porphyrin ring because porphyrin rings can slightly absorb the excitation light at 337 nm. In toluene, however, the emission from porphyrin rings was observed distinctly. The intensities were significantly higher than those of the emissions in acetonitrile and dichloromethane. Furthermore, the excitation spectra have a structure similar to the pyrene absorption structure in the wavelength region from 300 to 360 nm for Triads 2 and 3 (Fig. 8). These results suggest that energy transfer is the main process in toluene. The quantum yield of porphyrin fluorescence by pyrene excitation (Φ_3) is

$$\Phi_3 = \Phi_{ent}\Phi_1 \quad (2)$$

where Φ_{ent} is the quantum yield of energy transfer from the excited pyrene to the porphyrin moieties. Since the relative intensities of the pyrene peaks in the excitation spectra were smaller than the corresponding absorption peaks, Φ_{ent} is lower than unity. Φ_{ent} can be calculated by the following simple equation:

$$\Phi_{ent} = \frac{\Phi_3}{\Phi_1} \quad (3)$$

The Φ_{ent} values were 0.67 and 0.83 for Triad 2 and Triad 3, respectively.

Except for energy transfer, the relaxation is mainly electron transfer from excited pyrene to porphyrin. The electron transfer rate constant from pyrene (k_{elt}^{py}) is expressed by the following equation:

$$k_{elt}^{py} = \left(\frac{1}{\Phi_2} - \frac{1}{\Phi_0^{py}} - \frac{\Phi_{ent}}{\Phi_2}\right)\frac{\Phi_0^{py}}{\tau_0^{py}} \quad (4)$$

where Φ_2, Φ_0^{py} and τ_0^{py} are the fluorescence quantum yields for the pyrene moiety and the reference pyrene, and the fluorescence lifetime of the reference pyrene, respectively. This value is considered to be dependent on the pyrene–porphyrin distance (d), the free energy change ($-\Delta G_0(^1\mathrm{Py}^* \rightarrow \mathrm{CT})$) and the reorganization energy (λ). Although k_{elt}^{py} increases with decreasing d, no linearity between the logarithm of k_{elt}^{py} and d was observed as shown in Fig. 9. This character is similar to reductive electron transfer from photo-excited porphyrin. Apparent attenuation coefficients (β) for Triads 2 and 3 estimated in the same manner were 0.10 ± 0.12 Å^{-1}, which is of the same order as β for reductive electron transfer. These small β values for Triads 2 and 3 result from the partial overlap between the pyrene and the porphyrin moieties as mentioned in Section 3.2.

3.4. Factors governing the switching of energy transfer and electron transfer

The electron transfer rate can be controlled by solvents and pyrene–porphyrin distance (d) as mentioned above. The solvent dependencies of the energy transfer rate constants (k_{ent}^{py}) for excited pyrene are listed in Table 5. In the case of Triad 1 in all solvents, energetically allowed energy transfer was inhibited by the strong π–π interaction, which enhanced electron transfer. In Triads 2 and 3 with relatively large d, energy transfer and electron transfer coexisted and competed as relaxation processes in toluene, whereas oxidative electron transfer was the main process in acetonitrile and dichloromethane. Since the energy levels of the CT state become higher in a less polar solvent (Table 4), the energy levels of CT states in acetonitrile and dichloromethane (a relatively polar solvent) are lower than those in toluene (a relatively less polar solvent). However, destabilization

[4] The electron transfer rate depends on the energy gap $-\Delta G_0$ and the reorganization energy λ according to the Marcus theory [45,46]. As solvent polarity becomes larger, $-\Delta G_0$ (caused by decreasing the CT energy level) and λ become larger. $-\Delta G_0$ acts as a factor for enhancing the electron transfer rate. λ acts as a factor not only for enhancing but also for reducing the rate. The factor depending on $-\Delta G_0$ and λ is expressed by the following formula:

$$\frac{1}{\sqrt{4\pi\lambda k_B T}} \exp\left\{-\frac{(\Delta G_0 + \lambda)^2}{4\lambda k_B T}\right\}$$

The estimated values are 3.4 eV (acetonitrile), 3.6 eV (dichloromethane), and 0.54 eV (toluene) for Triad 2, and 1.9 eV (acetonitrile), 1.1 eV (dichloromethane), and 0.0062 eV (toluene) for Triad 3. These values mean that electron transfer is easier in acetonitrile and dichloromethane than in toluene in the present case.

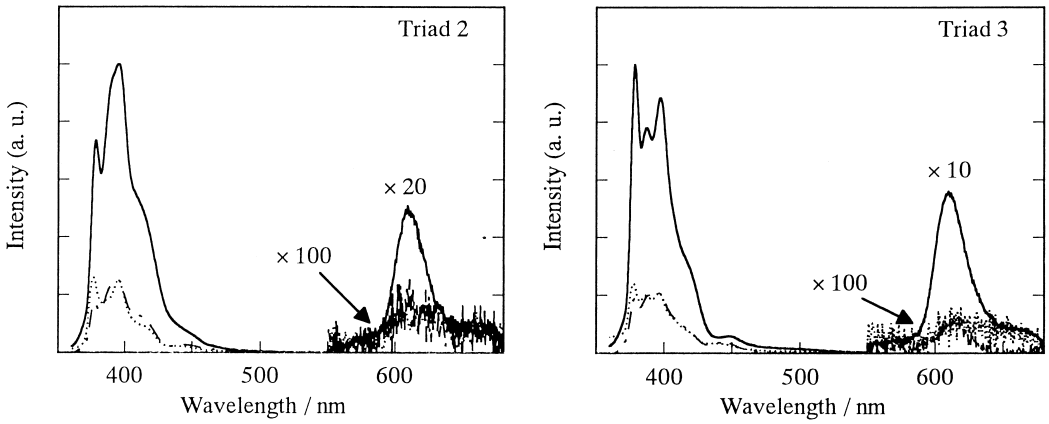

Fig. 7. The emission spectra of Triads 2 and 3 in toluene (solid), acetonitrile (dotted), and dichloromethane (chain) by excitation of the pyrene moieties ($\lambda_{ex} = 337$ nm).

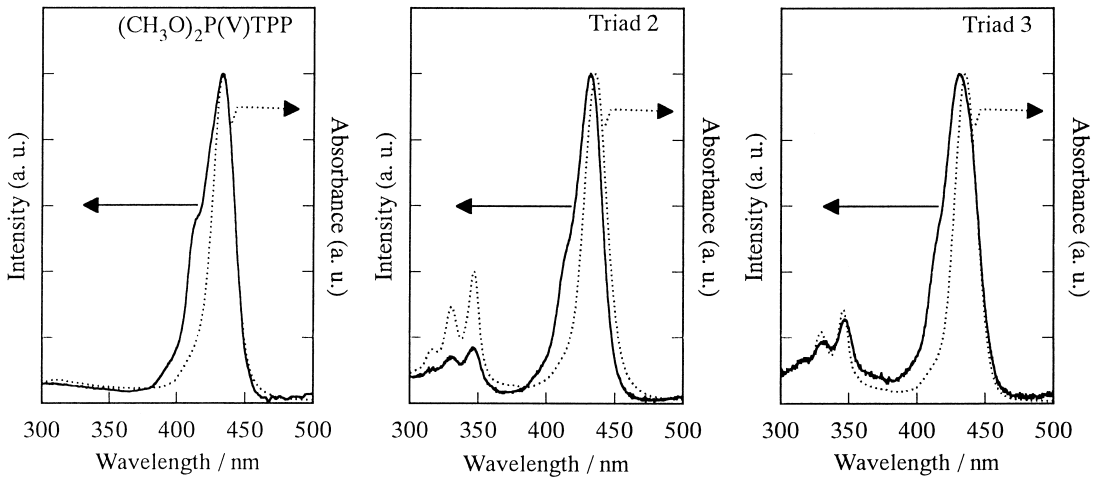

Fig. 8. The excitation spectra (solid) of porphyrin fluorescence and the absorption spectra (dotted) of $(CH_3O)_2P(V)TPP$, Triad 2, and Triad 3. The intensities were normalized at Soret peaks.

energy is not so large even in toluene, and E_{CT} cannot exist above E_{S1}^{py} and E_{S1}^{por}. In spite of such energetic estimation, energy transfer became the main process in toluene. In the case of photosynthetic reaction centers, it is known that the surroundings of a special pair are relatively less polar groups [1,2,3]. The less polar matrix is considered to be useful for

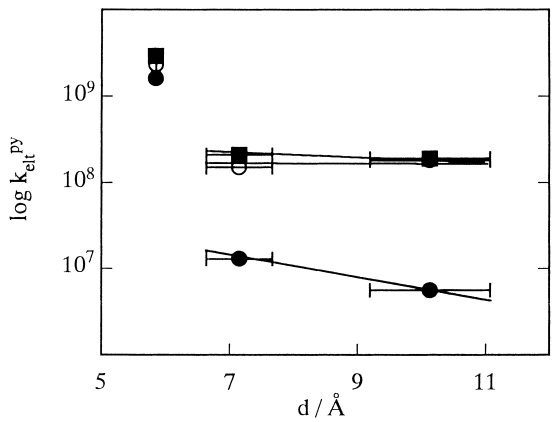

Fig. 9. The distance (d) dependence of the rate of electron transfer from excited pyrene to the porphyrin moieties (k_{elt}^{py}) in acetonitrile (■), dichloromethane (○), and toluene (●).

Table 5
Energy transfer and electron transfer properties of pyrene–porphyrin triads

Compounds	Solvent	k_{elt}^{Por} (10^8 s^{-1})	k_{elt}^{Py} (10^8 s^{-1})	k_{ent} (10^8 s^{-1})	Φ_{ent}
Triad 1	CH_3CN	x	290	nd	nd
	CH_2Cl_2	x	230	nd	nd
	Toluene	437	130	nd	nd
Triad 2	CH_3CN	114	21	trace	trace
	CH_2Cl_2	185	15	trace	trace
	Toluene	3.4	1.1	2.3	0.67
Triad 3	CH_3CN	38.5	19	trace	trace
	CH_2Cl_2	24.5	18	trace	trace
	Toluene	1.9	0.46	2.4	0.83

x: Too large.

the coexistence of energy transfer to the special pair and electron transfer from the special pair. On the other hand, the energy levels cannot explain their distance dependencies where the efficiency of energy transfer increases with increasing d. When energy transfer occurs through dipole–dipole interaction (Förster mechanism), the critical distance (R_0) is expressed by the following equation:

$$R_0^6 = \frac{9000\,\kappa^2 \Phi_0^{py} \ln 10}{128\pi^5 N n^4} \frac{\int F(\nu)\varepsilon(\nu)\nu^{-4}\,d\nu}{\int F(\nu)\,d\nu} \quad (5)$$

where κ, $F(\nu)$, $\varepsilon(\nu)$, ν, N, and n are the geometrical factor, the fluorescence intensity of the pyrene moiety, molar absorption coefficient of the porphyrin moiety, the wave number, the Avogadro constant, and the refractive index of the solvent, respectively [44].

When the geometry was assumed to be random orientation, R_0 was estimated at about 60 Å. This value means that the Förster-type energy transfer occurs easily in Triads 1–3. When energy transfer occurs only through the Förster mechanism, the quantum yields of energy transfer (Φ_{ent}) and electron transfer (Φ_{elt}^{py}) can be expressed by Eqs. (6) and (7), respectively:

$$\Phi_{ent} = \frac{1/\tau_0^{py}(d/R_0)^{-6}}{(1/\tau_0^{py}) + J\exp\{-\beta(d-d_0)\} + (1/\tau_0^{py})(d/R_0)^{-6}} \quad (6)$$

$$\Phi_{elt}^{py} = \frac{J\exp\{-\beta(d-d_0)\}}{(1/\tau_0^{py}) + J\exp\{-\beta(d-d_0)\} + (1/\tau_0^{py})(d/R_0)^{-6}} \quad (7)$$

where d_0, β, and τ_0^{py} are van der Waals radius, the attenuation coefficient of electron transfer, and the excited lifetime of pyrene, respectively. J is expressed by the Marcus equation [45,46] as follows:

$$J = \frac{4\pi^2}{h} V_0^2 \frac{1}{\sqrt{4\pi\lambda k_B T}} \exp\left\{-\frac{(\Delta G_0 + \lambda)^2}{4\lambda k_B T}\right\} \quad (8)$$

where h, V_0, λ, and ΔG_0 are Plank's constant, the transfer integral at $d = d_0$, the reorganization energy, and Gibbs free energy of the reaction, respectively. Curves calculated by these equations with various parameters are shown in Fig. 10, which demonstrates the dependence of the quantum yield of energy transfer (Φ_{ent}) on d, though this is just a qualitative explanation. Curves simulated against several J values with a fixed β value (Fig. 10(a)) and several β values with a fixed J value (Fig. 10(b)) qualitatively suggest that the character of Φ_{ent} increases as d become larger. However, a good fitting single curve could not be obtained for the results. One of the reasons for the mismatch is the greater J value for Triad 1, whose J value is much greater than those of Triads 2 and 3 due to strong π–π interaction between the pyrene and the porphyrin moieties (Fig. 10(a)). Another reason for the mismatch is the shortening of the actual pyrene–porphyrin distance from d by thermal fluctuation with flapping contact. Since the apparent β value (0.10 ± 0.12 Å^{-1}) calculated in Fig. 9 is too small to explain the results, the actual β value is considered to be the larger value and actual d is shortened by thermal fluctuation, as a result of which the correction of d along the arrows as shown in Fig. 10 is required. In addition, the other reasons for the mismatch supposedly are the exclusion of the Dexter-type energy transfer [47] and the constant $-\Delta G_0$, and λ used for all triads [45,46]. However, the present consideration gives an overall qualitative explanation of the switching between energy transfer and electron transfer.

4. Conclusions

In the photo-excited states of the pyrene or the porphyrin moieties, electron transfer occurred from the pyrene moieties to the porphyrin rings in the triads. In the photo-excited states of pyrene in Triads 2 and 3, energy transfer was observed in the less polar solvent. These phenomena indi-

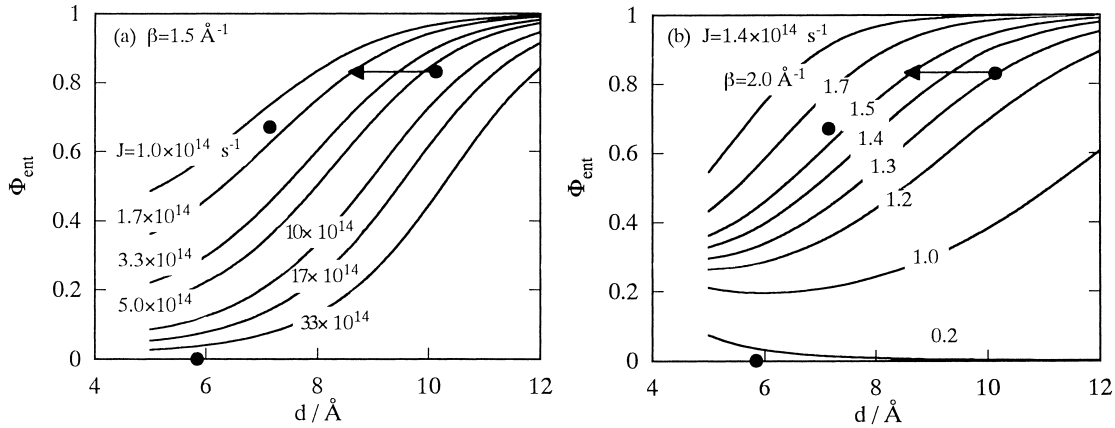

Fig. 10. The energy transfer quantum yield (Φ_{ent}) calculated by Eq. (6). The dependence on J value at fixed β value (a) and the dependence on β value at fixed J value (b).

cate that the switching between energy transfer and electron transfer is controlled by solvent polarity. The less polar matrix is considered to be useful for the coexistence of energy transfer and electron transfer. The efficiency of the energy transfer of the triads in less polar solvent increased with increasing pyrene–porphyrin distance (d). When assuming a Förster-type energy transfer, by which energy transfer was attenuated by d^{-6}, energy transfer became a major process in the region of large d because electron transfer was attenuated to an exponent of d. Although our explanation is only qualitative and a good fit could not be obtained by simple calculation, it provides a method to evaluate the photophysical switching of artificial molecular systems.

Acknowledgements

This work was partially supported by grants (Priority Area 282) from the Ministry of Education, Science and Culture of the Japanese Government and from the Japan Science and Technology Corporation.

References

[1] J. Breton, A. Vermeglio, (Eds.), The Photosynthetic Bacterial Reaction Center, Structure and Dynamics, Plenum Press, New York (London), 1988.
[2] J. Deisenhofer, H. Michel, Angew. Chem. Int. Ed. Engl. 28 (1989) 829.
[3] R. Huber, Angew. Chem. Int. Ed. Engl. 28 (1989) 848.
[4] G. Mcdermott, S.M. Prince, A.A. Freer, A.M. Hawthornthwaite-Lawless, M.Z. Papiz, R.J. Cogdell, N.W. Isaacs, Nature 374 (1995) 517.
[5] M.R. Wasielewski, Distance dependencies of electron transfer reactions, in: M.A. Fox, M. Chanon (Eds.), Photoinduced Electron Transfer, Elsevier, Ch. 1.4, Amsterdam, 1988, pp. 161–206.
[6] D. Gust, T.A. Moore, Science 244 (1989) 35.
[7] M.R. Wasielewski, Chem. Rev. 92 (1992) 435.
[8] M. Migita, T. Okada, N. Mataga, S. Nishitani, N. Kurata, Y. Sakata, S. Misumi, Chem. Phys. Lett. 84 (1981) 263.
[9] S. Nishitani, N. Kurata, Y. Sakata, S. Misumi, M. Migita, T. Okada, N. Mataga, Tetrahedron Lett. 22 (1981) 2099.
[10] N. Mataga, A. Karen, T. Okada, S. Nishitani, N. Kurata, Y. Sakata, S. Misumi, J. Phys. Chem. 88 (1984) 5138.
[11] A.R. Joran, B.A. Leland, G.G. Geller, J.J. Hopfield, P.B. Dervan, J. Am. Chem. Soc. 106 (1984) 6090.
[12] B.A. Leland, A.R. Joran, P.M. Felker, J.J. Hopfield, A.H. Zewail, P.B. Dervan, J. Phys. Chem. 89 (1985) 5571.
[13] A. Osuka, S. Morikawa, K. Maruyama, S. Hirayama, T. Minami, J. Chem. Soc., Chem. Commun. (1987) 359.
[14] A. Osuka, K. Maruyama, I. Yamazaki, N. Tamai, J. Chem. Soc., Chem. Commun. (1988) 1243.
[15] A. Osuaka, K. Maruyama, N. Mataga, T. Asahi, I. Yamazaki, N. Tamai, J. Am. Chem. Soc. 112 (1990) 4958.
[16] A. Osuka, K. Maruyama, I. Yamazaki, N. Tamai, Chem. Phys. Lett. 165 (1990) 392.
[17] A. Osuka, F. Kobayashi, K. Maruyama, N. Mataga, T. Asahi, T. Okada, I. Yamazaki, Y. Nishimura, Chem. Phys. Lett. 201 (1993) 223.
[18] Y. Sakata, H. Tsue, M.P. O'Neil, G.P. Wiederrecht, M.R. Wasielewski, J. Am. Chem. Soc. 116 (1994) 6904.
[19] M. Antolovich, P.J. Keyte, A.M. Oliver, M.N. Paddon-Row, J. Kroon, J.W. Verhoeven, S.A. Jonker, J.M. Warman, J. Phys. Chem. 95 (1991) 1933.
[20] D. Gust, T.A. Moore, A.L. Moore, C. Devadoss, P.A. Liddell, R. Hermant, R.A. Nieman, L.J. Demanche, J.M. DeGraziano, I. Gouni, J. Am. Chem. Soc. 114 (1992) 3590.
[21] A.N. Macpherson, P.A. Liddell, S. Lin, L. Noss, G.R. Seely, J.M. DeGraziano, A.L. Moore, T.A. Moore, D. Gust, J. Am. Chem. Soc. 117 (1995) 7202.
[22] A. Siemiarczuk, A.R. McIntosh, T.F. Ho, M.J. Stillman, K.J. Roach, A.C. Weedon, J.R. Bolton, J.S. Connolly, J. Am. Chem. Soc. 105 (1983) 7224.
[23] J.R. Bolton, T.F. Ho, S. Liauw, A. Siemiarczuk, C.S.K. Wan, A.C. Weedon, J. Chem. Soc., Chem. Commun. (1985) 559.
[24] M.R. Wasielewski, M.P. Niemczyk, J. Am. Chem. Soc. 106 (1984) 5043.
[25] M.R. Wasielewski, D.G. Johnson, M.P. Niemczyk, G.L. Gaines III, M.P. O'Neil, W.A. Svec, J. Am. Chem. Soc. 112 (1990) 6482.
[26] H. Segawa, K. Kunimoto, A. Nakamoto, T. Shimidzu, J. Chem. Soc., Perkin Trans. 1 (1992) 939.
[27] H. Segawa, N. Nakayama, T. Shimidzu, J. Chem. Soc., Chem. Commun. (1992) 784.
[28] H. Segawa, K. Kunimoto, K. Susumu, M. Taniguchi, T. Shimidzu, J. Am. Chem. Soc. 116 (1994) 11193.
[29] K. Susumu, K. Kunimoto, H. Segawa, T. Shimidzu, J. Photochem. Photobiol. A Chem. 92 (1995) 39.
[30] K. Susumu, H. Segawa, T. Shimidzu, Chem. Lett. (1995) 929.
[31] T.A. Rao, B.G. Maiya, J. Chem. Soc., Chem. Commun. (1995) 939.
[32] G.M. Stewart, M.A. Fox, J. Am. Chem. Soc. 118 (1996) 4354.
[33] C. Devadoss, P. Bharathi, J.S. Moore, J. Am. Chem. Soc. 118 (1996) 9635.
[34] F. Wilkinson, Competition between energy and electron transfer, in: M.A. Fox, M. Chanon (Eds.), Photoinduced Electron Transfer, Ch. 1.5, Elsevier, 1988, pp. 207–227.
[35] I.B. Beralman, Handbook of Fluorescence Spectra of Aromatic Molecules, Academic Press, New York (London), 1965.
[36] K. Susumu, K. Kunimoto, H. Segawa, T. Shimidzu, J. Phys. Chem. 99 (1995) 29.
[37] C.A. Marrese, C. Carrano, J. Inorg. Chem. 22 (1983) 1858.
[38] D. Mauzerall, Biochemistry 4 (1965) 1801.
[39] T.K. Chandrashekar, V. Krishnan, Bull. Soc. Chim. France (1984) 42.
[40] G.B. Maiya, V. Krishnan, J. Phys. Chem. 89 (1985) 5225.
[41] Z.M. Lin, W.Z. Feng, H.K. Leung, J. Chem. Soc., Chem. Commun. (1991) 209.
[42] E.S. Pysh, N.C. Yang, J. Am. Chem. Soc. 85 (1963) 2124.
[43] A. Weller, Z. Phys. Chem. Neue Folge 133 (1982) 93.
[44] Th. Förster, Ann. Physik. 6(2) (1948) 55.
[45] R.A. Marcus, J. Chem. Phys. 24 (1956) 966.
[46] R.A. Marcus, Annu. Rev. Phys. Chem. 15 (1964) 155.
[47] D.L. Dexter, J. Chem. Phys. 21 (1953) 836.